

# Broadband MMIC LNAs for ALMA Band 2+3 With Noise Temperature Below 28 K

David Cuadrado-Calle, *Member, IEEE*, Danielle George, *Member, IEEE*, Gary A. Fuller, Kieran Cleary, Lorene Samoska, *Senior Member, IEEE*, Pekka Kangaslahti, *Member, IEEE*, Jacob W. Kooi, *Member, IEEE*, Mary Soria, Mikko Varonen, *Member, IEEE*, Richard Lai, *Fellow, IEEE*, and Xiaobing Mei

**Abstract**—Recent advancements in transistor technology, such as the 35 nm InP HEMT, allow for the development of monolithic microwave integrated circuit (MMIC) low noise amplifiers (LNAs) with performance properties that challenge the hegemony of SIS mixers as leading radio astronomy detectors at frequencies as high as 116 GHz. In particular, for the Atacama Large Millimeter and Submillimeter Array (ALMA), this technical advancement allows the combination of two previously defined bands, 2 (67–90 GHz) and 3 (84–116 GHz), into a single ultra-broadband 2+3 (67–116 GHz) receiver. With this purpose, we present the design, implementation, and characterization of LNAs suitable for operation in this new ALMA band 2+3, and also a different set of LNAs for ALMA band 2. The best LNAs reported here show a noise temperature less than 250 K from 72 to 104 GHz at room temperature, and less than 28 K from 70 to 110 GHz at cryogenic ambient temperature of 20 K. To the best knowledge of the authors, this is the lowest wideband noise ever published in the 70–110 GHz frequency range, typically designated as *W*-band.

**Index Terms**—Atacama Large Millimeter and Submillimeter Array (ALMA), band 2+3, broadband, cryogenic, low noise amplifier (LNA), monolithic microwave integrated circuit (MMIC), 35 nm InP, *W*-band, WR-10.

Manuscript received October 10, 2016; revised November 28, 2016; accepted December 8, 2016. Date of publication January 30, 2017; date of current version May 4, 2017. This work was supported in part by the Science and Technology Facility Council (STFC) under Grant ST/LNST/L000768/1 and Grant ST/M003957/1, in part by the European Southern Observatory Program “Advanced Study for Upgrades of the Atacama Large Millimeter/Submillimeter Array,” and in part by the Jet Propulsion Laboratory, California Institute of Technology, under a contract with the National Aeronautics and Space Administration. The work of D. Cuadrado-Calle was supported by STFC under Grant ST/K502182/1.

D. Cuadrado-Calle and G. A. Fuller are with the Jodrell Bank Centre for Astrophysics, School of Physics and Astronomy, University of Manchester, Manchester M13 9PL, U.K. (e-mail: david.cuadradocalle@manchester.ac.uk).

D. George is with the School of Electrical and Electronics Engineering, The University of Manchester, Manchester M13 9PL, U.K. (e-mail: danielle.george@manchester.ac.uk).

K. Cleary is with the Department of Astronomy, California Institute of Technology, Pasadena, CA 91125 USA.

L. Samoska, P. Kangaslahti, J. W. Kooi, and M. Soria are with the Jet Propulsion Laboratory, California Institute of Technology, Pasadena, CA 91109 USA.

M. Varonen was with the Department of Micro and Nanoscience, Aalto University, 02150 Espoo, Finland. He is now with the VTT Technical Research Centre of Finland, 02044 Espoo, Finland.

R. Lai and X. Mei are with Northrop Grumman Aerospace Systems, Redondo Beach, CA 90278 USA.

Color versions of one or more of the figures in this paper are available online at <http://ieeexplore.ieee.org>.

Digital Object Identifier 10.1109/TMTT.2016.2639018

## I. INTRODUCTION

THE Atacama Large Millimeter and Submillimeter Array (ALMA) [1] is the largest astronomical project currently in existence. It is located in the Atacama Desert of Chile, in an area where the elevation, 5000 m, and atmospheric dryness create excellent conditions for performing astronomical observations in the millimeter and submillimeter frequency ranges. The telescope consists of 66 antennas, 54 with dishes of 12 m diameter and 12 with dishes of 7 m diameter, which are furnished with state-of-the-art front-end receivers in ten frequency bands, ranging from 31 to 950 GHz. Of particular interest for this paper are bands 2 and 3, whose technical specifications are listed in Table I.

ALMA employs HEMT low noise amplifiers (LNAs) as core detecting technology from 31 to 90 GHz, and SIS mixers from 84 GHz to the telescope’s upper observation limit of 950 GHz. However, with the most recent advancements in transistor fabrication technologies, particularly relating to InP HEMTs, it is possible to develop LNAs with excellent noise and wideband performance at frequencies as high as 116 GHz and beyond. This technical leap offers the prospect of combining bands 2 and 3 into a single ultra-broadband LNA-based receiver cartridge with a reduced cooling requirement of 20 K, instead of 4 K as required by SIS mixers. Furthermore, merging these two ALMA bands allows the inclusion of another receiver for a new frequency band, increasing the observational capability of the telescope.

This paper demonstrates the first LNAs suitable for operation in the 67–116 GHz frequency range with a noise temperature lower than the receiver specification shown in Table I. Moreover, the LNAs presented here are also suitable for future radio astronomy projects with broadband receivers in the *W*-band frequency range, such as the ngVLA [2] or LLAMA [3], and other non-astronomical applications such as automotive radars or millimeter wave imagers, which are of increasing demand in modern society [4].

## II. MMIC DESIGNS

This section presents two MMIC designs, one for band 2 and the other for band 2+3, which were developed using the state-of-the-art 35 nm gate length InP HEMT process of NGC [5]. This technology features a cutoff frequency greater than 400 GHz and a maximum transconductance (gm)

TABLE I  
ALMA BANDS 2 AND 3 SPECIFICATIONS

Band	Frequency range (GHz)	Receiver SSB noise specification (K) (80% band)	Maximum receiver SSB noise (K) (any RF frequency)
2	67–90	30	47
3	84–116	37	60

greater than 2200 mS/mm at a drain–source voltage ( $V_d$ ) of 1 V. The LNA chips were fabricated onto a 50  $\mu\text{m}$  thick InP substrate with through-substrate vias for grounding, 20 and 100  $\Omega/\text{sq}$  thin-film resistors, and 0.3 nF/mm<sup>2</sup> metal-insulator-metal capacitors. The transistors were passivated with a thin silicon nitride layer. Both MMIC designs consist of two transistor stages in common-source topology with the possibility of independent drain and gate biasing, and utilize 2-finger transistors whose total size (number of fingers  $\times$  finger width) is 60  $\mu\text{m}$  per stage. The MMIC design process was performed with individual simulation of the different matching networks using the electromagnetic (EM) simulator momentum, a tool included with the Keysight ADS package [6].

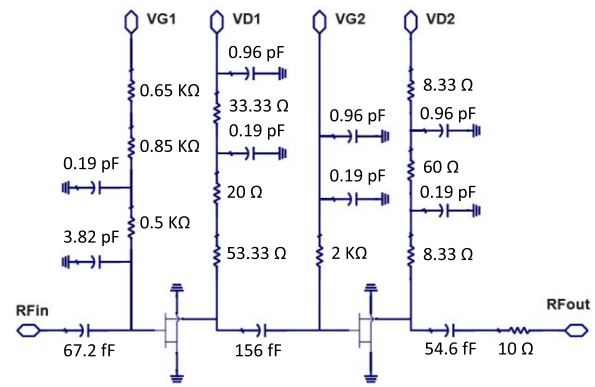
Figs. 1 and 2 show a simplified schematic of the MMICs, a microscopic photograph of the fabricated devices, and their simulated cryogenic performance, for the band 2 and 2+3 designs, respectively. The size of the fabricated chips was 1300  $\times$  900  $\mu\text{m}$  for both design types.

### III. MMICs CHARACTERIZATION

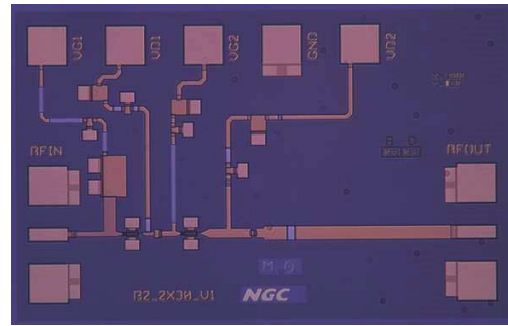
The fabricated wafers contained 13 MMICs of each design. Packaging and testing LNAs is a costly and time-consuming process, and for these reasons, the MMICs could not be picked blindly for packaging [7]. In order to select and package only the best chips, they were first tested in the cryogenic probe station at Caltech’s Cahill Radio Astronomy Laboratory (CRAL), which was configured to perform noise measurements in the 74–116 GHz frequency range at an ambient temperature of 20 K, as detailed in [8]. Utilization of this instrument allowed us to perform a relative comparison of the different fabricated MMICs, and determine which ones had the best noise performance. It must be emphasized that the tests performed with this instrument did not provide absolute noise temperature measurements because the contribution of the lossy input probe was not calibrated, resulting in a systematic overestimate of the absolute noise temperature.

Cryogenic probing tests were performed for 10 MMICs of each design type, with the transistors biased at a current density (drain current divided gate width) of 67 mA/mm. Fig. 3 shows a microscopic photograph of the process for probing a band 2 MMIC. The results of the tests are shown in Figs. 4 and 5 for band 2 and 2+3 MMICs, respectively.

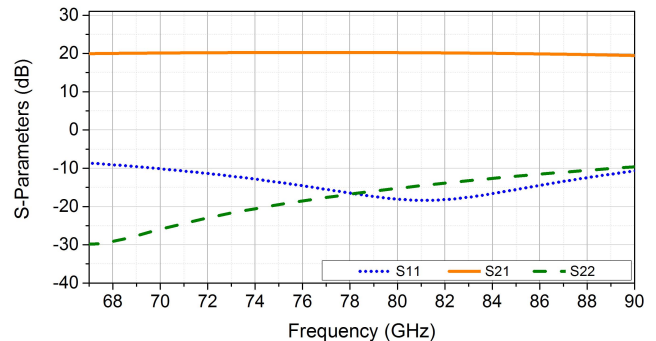
The yield of the band 2 and 2+3 MMIC designs can be estimated as 60% and 70%, respectively, at cryogenic temperature, based on the number of chips that did / did not turn on during the tests: 6/4 in the case of the band 2 design, and 7/3 in the case of the band 2+3 one. This is a result of both the fabrication process and the design parameters.



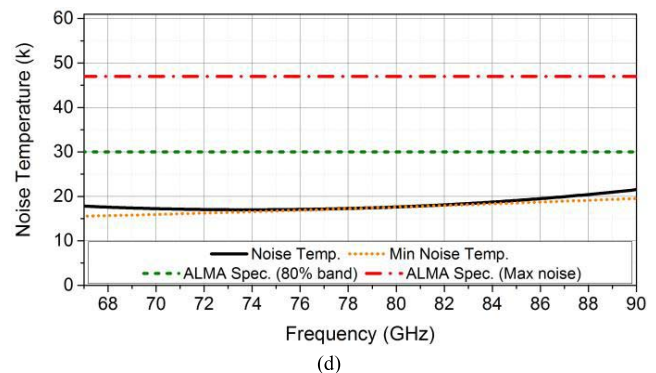
(a)



(b)



(c)

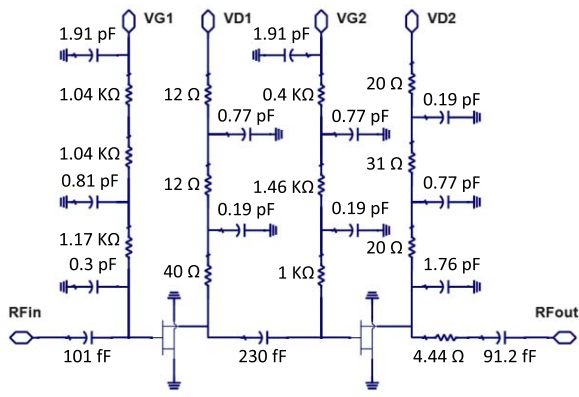


(d)

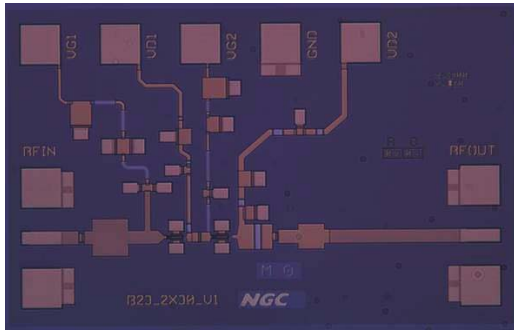
Fig. 1. MMIC design for ALMA band 2 (67 to 90 GHz). (a) Simplified schematic. (b) Microscopic photograph of a fabricated MMIC. (c) Simulated S-parameters at 20 K ambient temperature (simulated S12 is better than 34 dB from 67 to 90 GHz). (d) Simulated noise at 20 K ambient temperature plotted against ALMA specifications for receiver noise.

### IV. LNAs ASSEMBLY

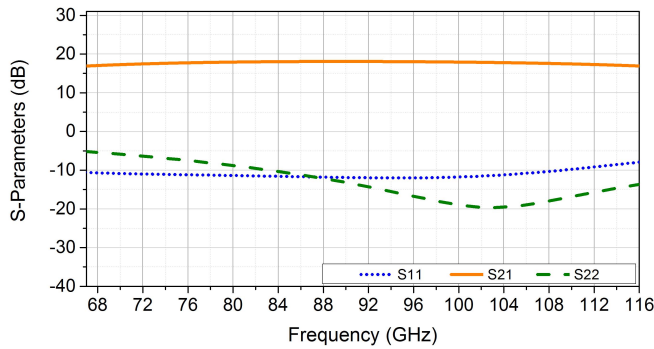
The best MMICs were selected and packaged in WR-10 blocks similar to that shown in Fig. 6, which were specifically



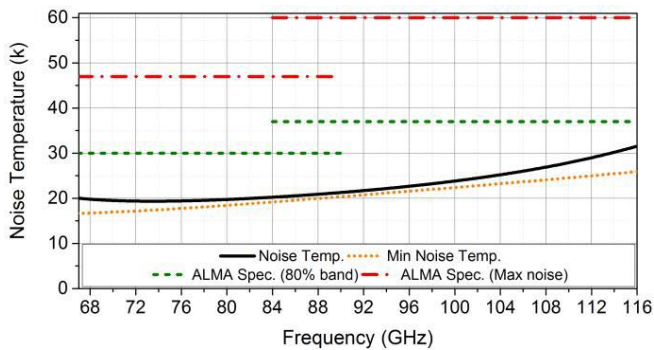
(a)



(b)



(c)



(d)

Fig. 2. MMIC design for ALMA band 2+3 (67 to 116 GHz). (a) Simplified schematic. (b) Microscopic photograph of a fabricated MMIC. (c) Simulated S-parameters at 20 K ambient temperature (simulated S12 is better than 30 dB from 67 to 116 GHz). (d) Simulated noise at 20 K ambient temperature plotted against ALMA specifications for receiver noise.

designed to cover the frequency range from 67 to 116 GHz. The WR-10 blocks were made of brass and gold plated with 5  $\mu\text{m}$  gold over 5  $\mu\text{m}$  nickel. Manufacture was in the

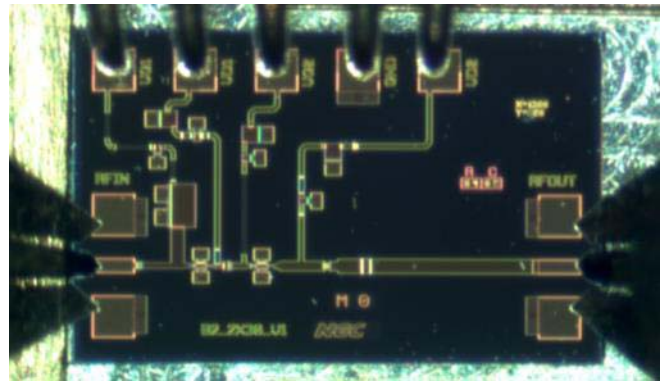


Fig. 3. Cryogenic probing of a band 2 MMIC.

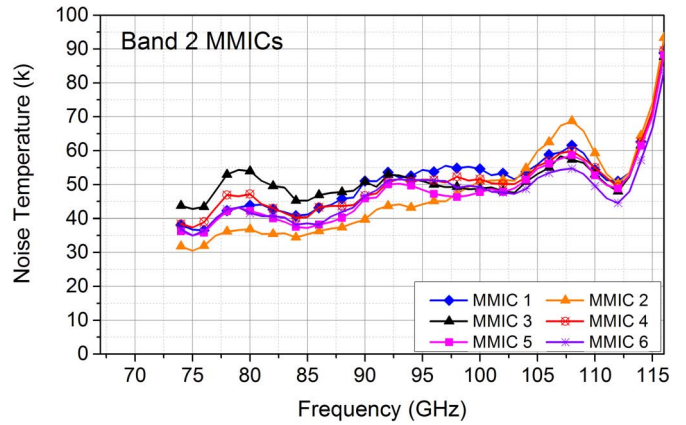


Fig. 4. Measured noise temperature of the band 2 MMICs tested in the cryogenic probe station. Not corrected for input probe contribution. Each trace corresponds to a different MMIC. Tests included four chips that did not turn on. Transistors were biased with a current density of 67 mA/mm.

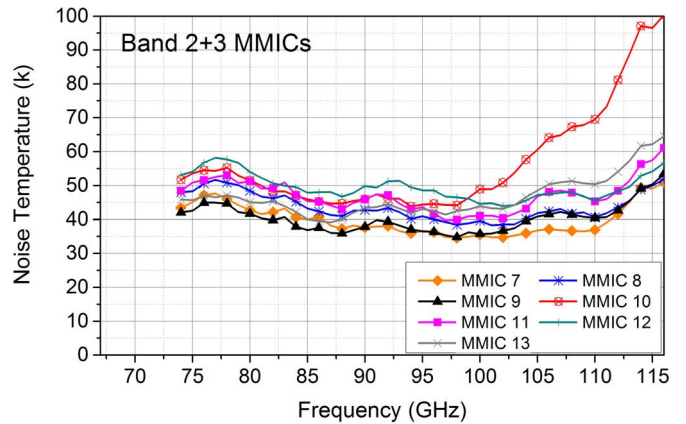


Fig. 5. Measured noise temperature of the band 2+3 MMICs tested in the cryogenic probe station. Not corrected for input probe contribution. Each trace corresponds to a different MMIC. Tests included three chips that did not turn on. Transistors were biased with a current density of 67 mA/mm.

mechanical workshops of the University of Manchester and the Rutherford Appleton Laboratory (RAL). The package was 3-D modeled with Autodesk Inventor [9], and EM simulated with Ansoft HFSS [10]. Table II gives the relationship of the MMICs packaged in each WR-10 block.

In order to couple the EM fields propagating along the waveguide channels to the microstrip lines at the input

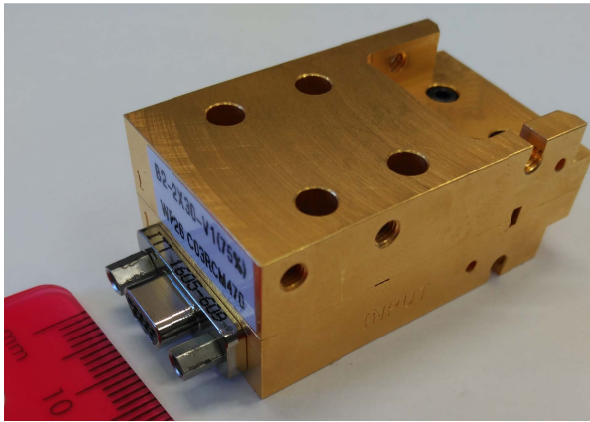


Fig. 6. Photograph of a WR-10 LNA block.

TABLE II  
PACKAGING OF THE MMICs IN WR-10 BLOCKS

WR-10 LNA reference	Chip reference	Design for ALMA band
B2a	MMIC 6	2
B2b	MMIC 2	2
B23a	MMIC 9	2+3
B23b	MMIC 8	2+3
B23c	MMIC 11	2+3
B23d	MMIC 13	2+3
B23e	MMIC 7	2+3

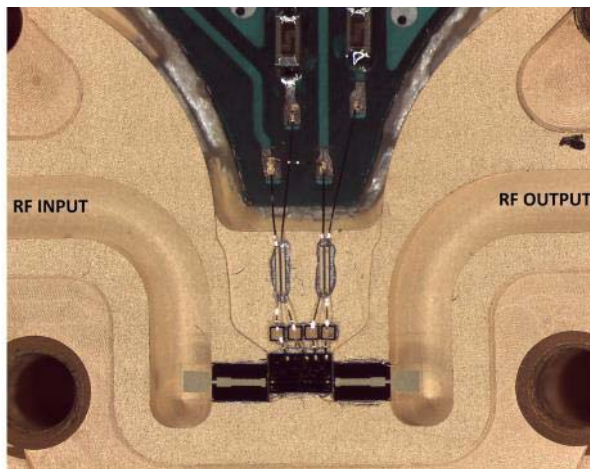


Fig. 7. Interior of a WR-10 LNA block.

and output of the MMICs, some *E*-plane waveguide-to-microstrip probes were specifically designed to operate in the 67–116 GHz frequency range, and manufactured. The fabricated probes can be seen in Fig. 7, which shows a photograph of one of the LNA blocks with the cover removed. Fig. 8 shows the simulated reflection coefficient of the probes from the MMIC side plotted against the simulated optimum reflection coefficient ( $\Gamma_{\text{opt}}$ ) of the MMICs. The design of the probes was done with the EM simulator Ansoft HFSS, and fabrication material was 3 mil thick quartz substrate with 3  $\mu\text{m}$  gold on both sides. Quartz is regarded as a suitable material for this application due to its low dielectric constant ( $\epsilon_r$ ) of 3.8.

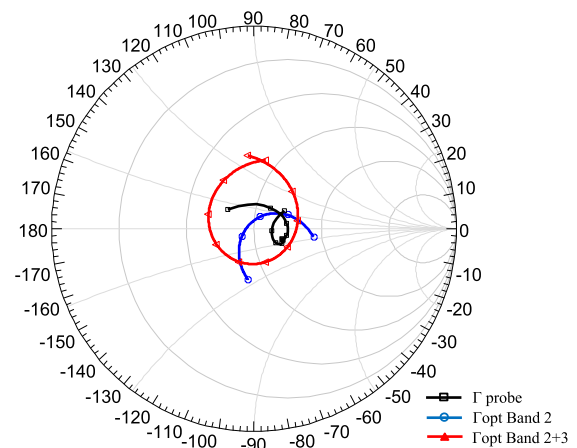


Fig. 8. Smith chart plots of simulated: input reflection coefficient of the waveguide-to-microstrip probes from the MMIC side in the 67–116 GHz range (black line with rectangles),  $\Gamma_{\text{opt}}$  of the band 2 MMIC design (blue line with circles) in the 67–90 GHz range, and  $\Gamma_{\text{opt}}$  of the band 2+3 MMIC design (red line with triangles) in the 67–116 GHz range.

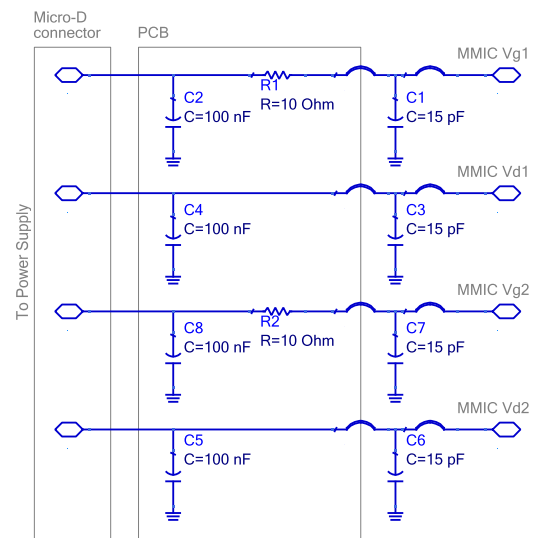


Fig. 9. Off-chip bias protection circuit.

In addition, it is transparent and so allows for an easy alignment of the probes and removal of the excess epoxy in the waveguide channel.

Biasing of the transistors in the MMIC was done through a 9-pin micro-D connector embedded in the WR-10 blocks. LNAs are devices that operate at low voltages and are susceptible to damage from electrostatic discharge and improper biasing, as well as being sensitive to low-level interference [11]. For this reason, a protection circuit was included in the form of a PCB and some bondable decoupling capacitors close to the MMIC. The schematic of this circuit is shown in Fig. 9.

## V. LNAs CHARACTERIZATION

The LNAs were characterized at room temperature for S-parameters and noise, and at cryogenic ambient temperature of 20 K for noise. Tests were done at the CRAL. The S-parameters were tested with a Rohde and Schwarz ZVA 24 Vector Network Analyzer, and ZVA-Z110 WR-10 converter head extensions. Noise characterization of the LNAs was performed by application of the Y-factor method, according to the

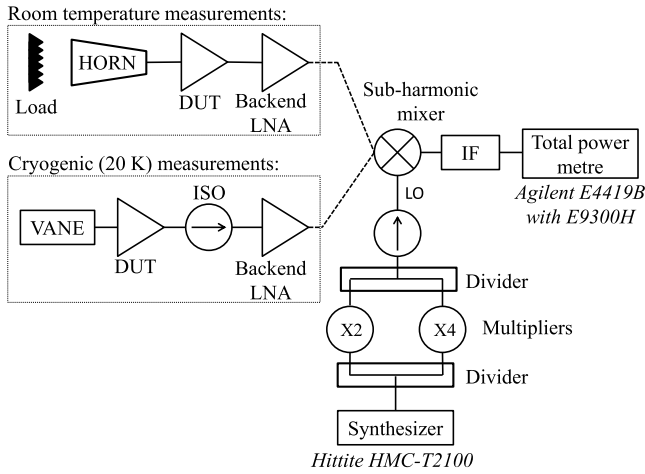


Fig. 10. Test setup for noise characterization at room temperature (295 K) and cryogenic temperature (20 K). DUT is the device (LNA) under test. X2 and X4 multipliers were turned ON/OFF with a LabVIEW vi interface, and only one was active at a time. The subharmonic mixer is the part WR10SHM from Virginia diodes.

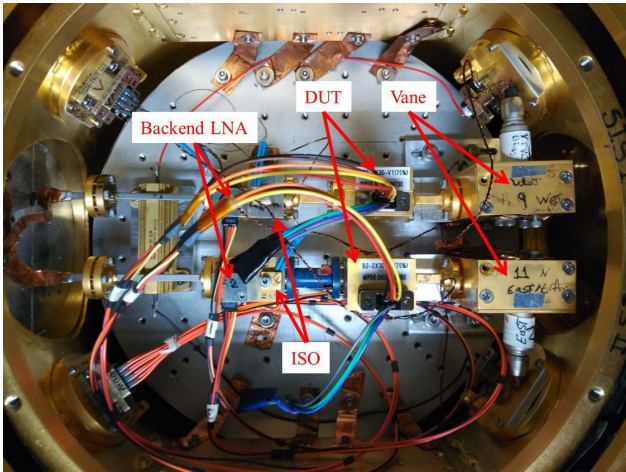


Fig. 11. Interior of the Dewar with setup for characterizing two LNA blocks.

test bench diagram shown in Fig. 10, and applying a correction to subtract the noise contribution of the back-end. For the room temperature measurements, the DUT LNA was attached to a rectangular horn, and the Y-factor method was applied with external 290 K “hot” and 77 K “cold” loads. For the noise characterization of the LNAs at cryogenic temperature, the DUT and the back-end LNA were inserted into a 20 K closed cycle cryostat, whose interior is shown in Fig. 11. In this case, the input of the DUT was attached to a variable temperature vane, configured to present “hot” and “cold” loads of 75 K and 25 K, respectively, at the input of the LNA. The results from these tests are presented in Fig. 12 for the ALMA band 2 LNAs and in Fig. 13 for the ALMA band 2+3 LNAs. The estimated random uncertainty of the cryogenic noise measurements is  $\pm 1.6$  K ( $\sigma$ ), based on the scatter of the IF power measurements and the uncertainty of the temperature sensor in the vane. This is consistent with the peak-to-peak scatter of  $\pm 1.9$  K across the 75–105 GHz band for B23a (the device with the most uniform performance across this band). In addition, we estimate a potential systematic offset of up to  $\pm 2.7$  K based on the accuracy of the power sensor and

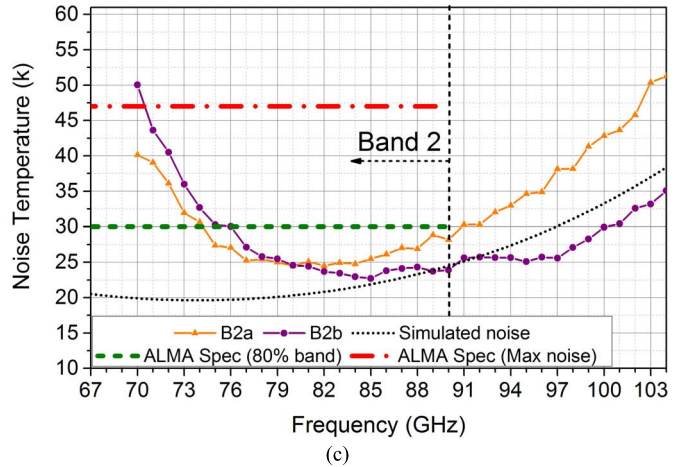
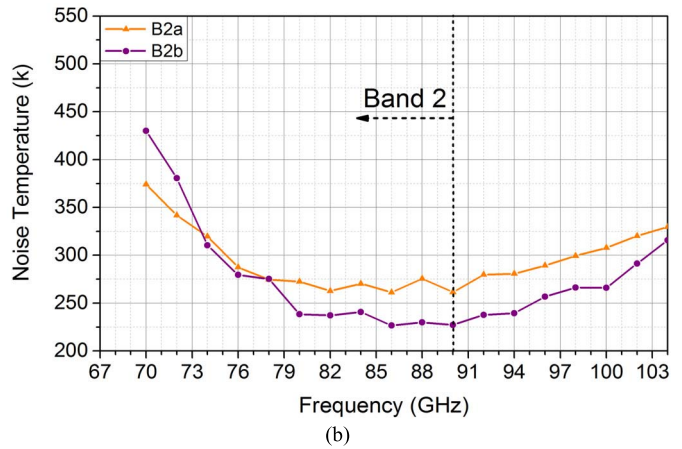
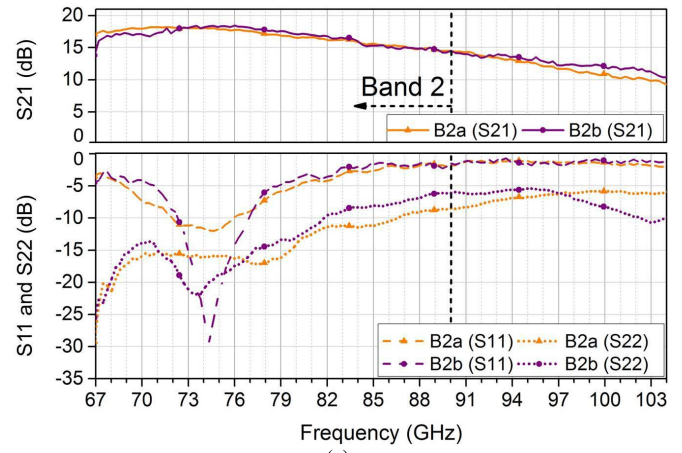


Fig. 12. Characterization of two WR-10 LNA blocks for ALMA band 2. Blocks are designated as B2a and B2b. Transistors were biased with a current density of 167 mA/mm for the room temperature measurements and 75 mA/mm for the cryogenic measurements. (a) Measured S-parameters at ambient temperature of 295 K. (b) Measured noise temperature at ambient temperature of 295 K. (c) Measured noise temperature at ambient temperature of 20 K plotted against specifications for ALMA receiver noise and simulated noise assuming 0.3 dB package loss prior to the MMIC.

the power/temperature loss in the waveguide section between the vane and the DUT.

It was experimentally determined that the best performance was obtained biasing the band 2 LNAs with a current density of 167 mA/mm at room temperature and 75 mA/mm at cryogenic temperature, and the band 2+3 LNAs with a current density of 200 mA/mm at room temperature and 67mA/mm

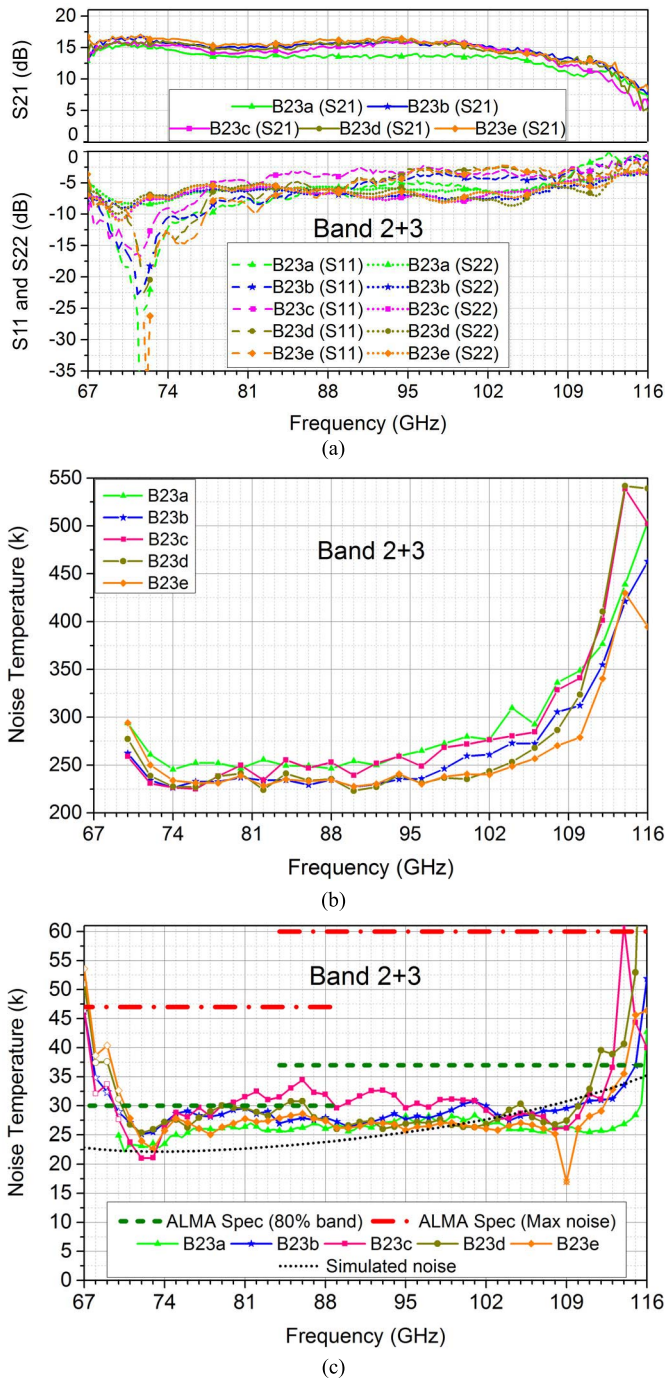


Fig. 13. Characterization of five WR-10 blocks for ALMA band 2+3. Blocks are designated as B23a, B23b, B23c, B23d, and B23e. Transistors were biased with a current density of 200 mA/mm for the room temperature measurements and 67 mA/mm for the cryogenic measurements. (a) Measured S-parameters at ambient temperature of 295 K. (b) Measured noise temperature at ambient temperature of 295 K. (c) Measured noise temperature at ambient temperature of 20 K plotted against ALMA specifications for receiver noise and simulated noise assuming 0.3 dB package loss prior to the MMIC. Samples with no color filling below 70 GHz were measured with a WR12 mixer (WR12SHM) instead of a WR10 one as described in Fig. 10. We believe the spike at 109 GHz in the cryogenic noise temperature of B23e may be due to an error in the measurement system.

at cryogenic temperature. With these biasing conditions the power consumption at cryogenic temperature is 10 mW in the case of the band 2 LNAs, and 6 mW in the case of the band 2+3 LNAs.

## VI. DISCUSSION OF RESULTS

In the previous section, the results of the LNA characterization were presented. From Fig. 12, it can be observed that the LNAs for ALMA band 2 (B2a and B2b) have very similar performance up to 82 GHz. However, the noise performance of B2b is superior in the 82–90 GHz range. As previously described, these LNAs for ALMA band 2 were designed to operate from 67 to 90 GHz. In this band, B2b has a room temperature gain of  $16.5 \pm 1.5$  dB, and noise temperature between 225 and 430 K at room temperature and between 23 and 50 K at a cryogenic temperature of 20 K. Moreover, it is interesting to point out that B2b also has good performance from 90 to 100 GHz, featuring a cryogenic noise temperature of less than 30 K.

Concerning the LNAs for ALMA band 2+3, Fig. 13 shows that B23d and B23e achieve a noise temperature less than 250 K from 72 to 104 GHz at room temperature, and B23a and B23e show a cryogenic noise temperature less than 28 K from 70 to 110 GHz. We believe these results show the lowest broadband noise temperature so far reported for LNAs operating at W-band, and this is supported by a comparison with other state-of-the-art works from the literature in Table III.

Table IV is also provided to compare the noise performance of the LNAs with the specifications for receiver noise in five frequency bands of interest for ALMA. As described in Section I, these specifications are for maximum noise over 80% of the RF bandwidth, and maximum noise at any RF frequency. The frequency bands of study include the previously described bands 2, 3, and 2+3, and two alternative ones that we propose and designate as “extended band 2” (68 to 100 GHz) and “reduced band 2+3” (68 to 114 GHz). The noise specifications for these two alternative bands are not an official ALMA specification, and were calculated as a pro-rated average between the specifications for bands 2 and 3, as

$$\text{Spec(K)} = \frac{\text{BW}_{B2}(\text{GHz}) \cdot \text{Spec}_{B2}(\text{K})}{\text{BW}_{\text{TOTAL}}(\text{GHz})} + \frac{\text{BW}_{B3}(\text{GHz}) \cdot \text{Spec}_{B3}(\text{K})}{\text{BW}_{\text{TOTAL}}(\text{GHz})} \quad (1)$$

where BW and Spec are the bandwidth and noise specification of the corresponding frequency band.

It can be observed that although the band 2 LNAs have a noise performance comparable to other state-of-the-art devices in the same frequency range, they do not fully meet the ALMA specifications. This is due to their noise performance in the lower end of the band, from 67 to 73 GHz, which is higher than expected from the simulations.

We demonstrate on the other hand that the ALMA band 2+3 design presents a noise temperature lower than the ALMA receiver specifications for band 2, and significantly exceeds the specifications for band 3. This is best exemplified through the LNAs B23a, B23b, and B23e, which have a noise temperature less than 31 K over 80% of the bandwidth from 67 to 116 GHz, and less than 54 K at any RF frequency in the same range. The performance of these band 2+3 LNAs proves that it is possible to develop ultra-low noise W-band amplifiers with a relative bandwidth as high as 54%, and opens the door to a new generation of ultra-wideband radio astronomy receivers.

TABLE III  
COMPARISON WITH STATE-OF-THE-ART LNAs FROM THE LITERATURE

Freq. Range [GHz]	Gain (room temperature) [dB]	Noise (room temperature) min – max [K]	Noise (cryogenic temperature) min – max [K]	Process	MIC/MMIC	Work Reference
70 – 100	15.5 ± 3	225 – 430	23 – 50	35 nm InP pHEMT	MMIC	This work (B2b)
67 – 114	13 ± 3	246 – 438 <sup>(2)</sup>	22 – 28 <sup>(2)</sup>	35 nm InP pHEMT	MMIC	This work (B23a)
68 – 113	14 ± 2	227 – 385 <sup>(2)</sup>	25 – 35	35 nm InP pHEMT	MMIC	This work (B23b)
68 – 113	14.5 ± 2.5	227 – 385 <sup>(2)</sup>	22 – 40	35 nm InP pHEMT	MMIC	This work (B23e)
67 – 90	28 ± 2	270 – 400	22 – 52	35 nm InP pHEMT	MMIC	[12]
75 – 110	13 ± 3	180 – 260	27 – 35	35 nm InP pHEMT	MMIC	[13]
75 – 110	15 ± 4	nr <sup>(1)</sup>	25 – 35	35 nm InP pHEMT	MMIC	[14]
75 – 110	27 ± 2	nr <sup>(1)</sup>	24 – 40	35 nm InP pHEMT	MMIC	[14]
75 – 116	22 ± 3	230 – 350	24 – 39	35 nm InP pHEMT	MMIC	[15]
75 – 116	21.5 ± 3.5	240 – 320	26 – 48	35 nm InP pHEMT	MMIC	[16]
70 – 110	23 ± 3	250 – 330	nr <sup>(1)</sup>	70 nm GaAs mHEMT	MMIC	[17]
80 – 100	18.5 ± 3	225 – 295	nr <sup>(1)</sup>	70 nm GaAs mHEMT	MMIC	[18]
75 – 110 <sup>(3)</sup>	18.5 ± 2.5	180 – 262	nr <sup>(1)</sup>	50 nm GaAs mHEMT	MMIC	[19]
60 – 90	22 ± 2	159 – 225	nr <sup>(1)</sup>	50 nm GaAs mHEMT	MMIC	[20]
60 – 80	16 ± 2	200 – 300	45 – 90	100 nm InP HEMT	MIC	[21]

<sup>(1)</sup> nr = not reported.

<sup>(2)</sup> Not tested from 67 GHz to 70 GHz.

<sup>(3)</sup> MMIC measurements only.

TABLE IV  
CRYOGENIC NOISE PERFORMANCE OF THE LNAs VERSUS ALMA SPECIFICATIONS

	ALMA band	Band 2 LNAs		Band 2+3 LNAs					ALMA receiver specification (K)
		B2a <sup>(1)</sup>	B2b <sup>(1)</sup>	B23a <sup>(1)</sup>	B23b	B23c	B23d	B23e	
Max noise over 80% bandwidth (K)	Band 2 (67-90 GHz)	32	36	26	29	32	31	29	30
	Ext. Band 2 (68-100 GHz)	38	30	27	29	32	30	28	32 <sup>(2)</sup>
	Band 3 (84-116 GHz)	-	-	28	31	33	31	28	37
	Red. Band 2+3 (68-114 GHz)	-	-	27	30	32	31	28	34 <sup>(2)</sup>
	Band 2+3 (67-116 GHz)	-	-	27	31	33	31	29	34 <sup>(2)</sup>
Maximum noise at any RF frequency (K)	Band 2 (67-90 GHz)	40	50	27	46	46	51	54	47
	Ext. Band 2 (68-100 GHz)	43	50	28	35	34	38	40	51 <sup>(2)</sup>
	Band 3 (84-116 GHz)	-	-	43	52	61	113	46	60
	Red. Band 2+3 (68-114 GHz)	-	-	28	35	61	41	40	54 <sup>(2)</sup>
	Band 2+3 (84-116 GHz)	-	-	43	52	61	113	54	54 <sup>(2)</sup>

Font color indicates if the noise of the LNA is below the receivers' specification. Green: yes. Orange: no by less than 10%. Red: no by more than 10%.

<sup>(1)</sup> Not tested from 67 GHz to 70 GHz.

<sup>(2)</sup> Specification for receiver noise in extended band 2, reduced band 2+3, and band 2+3 calculated as the prorated average between bands 2 and 2+3 in the frequency range of interest: Noise (K) =  $(BW_{B2} / BW_{TOTAL}) * Spec_{B2} + (BW_{B3} / BW_{TOTAL}) * Spec_{B3}$ . This is not an official ALMA specification, and it's subject to the authors' interpretation.

This provides considerable benefit to future radio astronomy where wide-bandwidth observations will be required [22].

## VII. CONCLUSION

In this paper, we presented the design and implementation of two cryogenic LNA designs suitable for operation in the frequency ranges of ALMA band 2 (67 to 90 GHz), and a new combined band 2+3 (67 to 116 GHz). We showed the characterization results of two fully assembled WR-10 LNAs for band 2 and five for band 2+3. Some of these LNAs showed a noise temperature less than 250 K from 72 to 104 GHz at room temperature, and less than 28 K across all of *W*-band

(70 to 110 GHz) at cryogenic ambient temperature of 20 K. After performing a comparison with other state-of-the-art works from the literature, we demonstrated that these LNAs establish a new record for broadband noise in *W*-band.

## ACKNOWLEDGMENT

The authors would like to thank the contributions of A. Galtress (Jodrell Bank) to the design of the WR-10 bodies and A. Baiza (JPL) to the assembly of the LNAs. They would also like to thank Prof. B. Ellison (RAL), Dr. R. Gawande (JPL), Dr. W. McGenn (University of Manchester), and Dr. S. Rea (RAL) for helpful discussions.

## REFERENCES

- [1] A. Wootten and A. R. Thompson, "The atacama large millimeter/submillimeter array," *Proc. IEEE*, vol. 97, no. 8, pp. 1463–1471, Aug. 2009.
- [2] C. L. Carilli *et al.* (Oct. 2015). "Next generation very large array memo no. 5: Science working groups—Project overview." [Online]. Available: <https://arxiv.org/abs/1510.06438>
- [3] E. M. Arnal *et al.*, "LLAMA observatory," IV LAPIS International School–Millimeter/Submillimeter Astronomy With LLAMA. (Aug. 2012). [Online]. Available: <http://www.iar.unlp.edu.ar/llama-web/presentaciones.htm>
- [4] G. M. Brooker, "Millimetre wave radar for tracking and imaging applications," in *Proc. 1st Int. Conf. Sens. Technol.*, 2005, pp. 158–163.
- [5] R. Lai *et al.*, "Sub 50 nm InP HEMT device with Fmax greater than 1 THz," in *Proc. IEEE Electron Devices Meeting*, Washington, DC, USA, Dec. 2007, pp. 609–611.
- [6] ADS, *Keysight, version 2015.01*.
- [7] R. Reeves *et al.*, "Cryogenic probing of mm-wave MMIC LNAs for large focal-plane arrays in radio-astronomy," in *Proc. Eur. Microw. Integr. Circuit Conf. (EuMIC)*, 2014, pp. 580–583.
- [8] D. Russell, K. Cleary, and R. Reeves, "Cryogenic probe station for on-wafer characterization of electrical devices," *Rev. Sci. Instrum.*, vol. 83, no. 4, p. 044703, 2012.
- [9] *Inventor, Autodesk*, 2016.
- [10] HFSS, *Ansoft, version 13.0*.
- [11] J. W. Lamb, "Evaluation of biasing and protection circuitry components for cryogenic MMIC low-noise amplifiers," *Cryogenics*, vol. 61, pp. 43–54, May/June 2014.
- [12] E. W. Bryerton *et al.*, "A W-band low-noise amplifier with 22K noise temperature," in *IEEE MTT-S Int. Microw. Symp. Dig.*, Jun. 2009, pp. 681–684.
- [13] L. Samoska *et al.*, "Cryogenic MMIC low noise amplifiers for W-band and beyond," in *Proc. NRAO ISSTT Session*, vol. 10, 2011, pp. 193–196.
- [14] L. Samoska *et al.*, "W-band cryogenic InP MMIC LNAs with noise below 30K," in *IEEE MTT-S Int. Microw. Symp. Dig.*, Jun. 2012, pp. 1–3.
- [15] M. Varonen *et al.*, "A 75–116–GHz LNA with 23-K noise temperature at 108 GHz," in *IEEE MTT-S Int. Microw. Symp. Dig.*, Jun. 2013, pp. 1–3.
- [16] M. Varonen *et al.*, "An MMIC low-noise amplifier design technique," *IEEE Trans. Microw. Theory Techn.*, vol. 64, no. 3, Mar. 2016, pp. 826–835.
- [17] *Preliminary Datasheet CGY2190UH/C2, OMMIC*, 2011.
- [18] C. Schwörer, A. Tessmann, A. Leuther, H. Massler, W. Reinert, and M. Schlechtweg, "Low-noise W-band amplifiers for radiometer applications using a 70 nm metamorphic HEMT technology," in *Proc. 11th Gallium Arsenide Appl. Symp. (GAAS)*, Munich, Germany, 2003, pp. 373–376.
- [19] F. Thome *et al.*, "Comparison of two W-band low-noise amplifier MMICs with ultra low power consumption based on 50nm InGaAs mHEMT technology," in *IEEE MTT-S Int. Microw. Symp. Dig.*, Jun. 2013, pp. 1–4.
- [20] P. M. Smith *et al.*, "A 50nm MHEMT millimeter-wave MMIC LNA with wideband noise and gain performance," in *IEEE MTT-S Int. Microw. Symp. Dig.*, Jun. 2014, pp. 1–4.
- [21] M. W. Pospieszalski *et al.*, "Millimeter-wave, cryogenically-coolable amplifiers using AlInAs/GaInAs/InP HEMTs," in *IEEE MTT-S Int. Microw. Symp. Dig.*, vol. 2, Jun. 1993, pp. 515–518.
- [22] D. Cuadrado-Calle, D. George, B. Ellison, G. A. Fuller, and K. Cleary, "Low noise amplifiers, the future for millimetre-wave radio astronomy receivers?" accepted for publication.



**David Cuadrado-Calle** (M'13) received the B.Sc. and M.Sc. degrees in communications engineering from the University of Alcalá, Alcalá de Henares, Spain, in 2010 and 2012, respectively. He is currently pursuing the Ph.D. degree at The University of Manchester, Manchester, U.K.

In 2011, he joined Yebes Observatory, Yebes, Spain, where he was involved in the development of RF instrumentation for the 40 and 13 m telescopes. From 2012 to 2013, he was an RF Engineer at the private sector in Spain. His Ph.D. project consists of the development of MMIC LNAs for ALMA band 2+3 and other radio astronomy projects. From 2015 to 2016, he was a Visiting Ph.D. Researcher for six months with the California Institute of Technology, Pasadena, CA, USA, and NASA's Jet Propulsion Laboratory, Pasadena.



**Danielle George** (M'04) is currently a Professor of RF and microwave communication engineering with The University of Manchester, Manchester, U.K., where she is the Vice Dean for teaching and learning with the Faculty of Science and Engineering. She is involved in solving one of the 14 world engineering grand challenges of the 21st Century. She engineers tools for scientific discovery. Her current research interests include the design of low-noise amplifiers and communication systems for space and aerospace sectors.



**Gary A. Fuller** received the Ph.D. degree from the Astronomy Department, University of California, Berkeley, CA, USA.

He was a Pre-Doctoral Fellow with the Harvard-Smithsonian Center for Astrophysics (CfA), Cambridge, MA, USA. He was a Smithsonian Post-Doctoral Fellow with CfA and a Jansky Fellow with the National Radio Astronomy Observatory, Tucson, AZ, USA, and National Radio Astronomy Observatory, Charlottesville, VA, USA. He is currently a Professor of astrophysics with the Jodrell Bank Centre for Astrophysics (JBCA), School of Physics and Astronomy, The University of Manchester, Manchester, U.K., and he is a Principal Investigator and a Lead Scientist of the UK ALMA Regional Centre Node, JBCA. His current research interests include understanding the formation and early evolution of stars in our galaxy and other galaxies.



**Kieran Cleary** received the M.Eng.Sc. degree in electronic engineering from the National University of Ireland, Dublin, Ireland, in 1994, and the Ph.D. degree in radio astronomy (on cosmic microwave background observations using the Very Small Array) from The University of Manchester, Manchester, U.K., in 2004.

From 2004 to 2006, he was a Post-Doctoral Scholar with the Jet Propulsion Laboratory, California Institute of Technology, Pasadena, CA, USA, where he was involved in the properties of powerful radio galaxies using the Spitzer Space Telescope. Since 2006, he has been with the California Institute of Technology, where he is currently a Senior Staff Scientist, involved in an experiment to measure redshifted carbon monoxide emission from the epoch of galaxy assembly, as well as leading the Cahill Radio Astronomy Laboratory.



**Lorene Samoska** (M'95–SM'04) received the B.S. degree in engineering physics from the University of Illinois, Urbana-Champaign, IL, USA, in 1989, and the Ph.D. degree in materials engineering from the University of California (UC), Santa Barbara, CA, USA, in 1995.

She was a Post-Doctoral Researcher with UC, where she was involved in the design and fabrication of state-of-the-art InP HBT microwave digital circuits. She joined the Jet Propulsion Laboratory, Pasadena, CA, USA, in 1998, where she is currently a Principal Engineer, involved in the design and testing of 30–600 GHz HEMT MMIC low-noise amplifiers and receivers, power amplifiers for local oscillator sources, and transmitters in future space missions.



**Pekka Kangaslahti** (S'94–M'98) received the M.Sc. and Ph.D. degrees from Aalto University (formerly the Helsinki University of Technology), Espoo, Finland, in 1992 and 1999, respectively.

He is currently a Principal Engineer with the Microwave Systems Technology Group, Jet Propulsion Laboratory, California Institute of Technology, Pasadena, CA, USA. His current research interests include the development of millimeter-wave, submillimeter-wave, and monolithic microwave integrated circuits, modules, receivers, and receiver

arrays.



**Jacob W. Kooi** (M'02) was born in Geldrop, The Netherlands, in 1960. He received the B.S. degree in microwave engineering from California Polytechnic State University, San Luis Obispo, CA, USA, in 1985, the M.S. degree in electrical engineering from the California Institute of Technology, Pasadena, CA, USA, in 1992, and the Ph.D. degree in physics from the University of Groningen, Groningen, The Netherlands, in 2008.

Since 2014, he has been an Instrument Scientist with the Microwave Remote Sensing Instrument

Division, Jet Propulsion Laboratory, California Institute of Technology. His current research interests include millimeter-wave and submillimeter-wave technology, low-energy physics, electrodynamics, thermodynamics, low-noise amplifiers and associated monolithic microwave integrated circuit technology, Fourier optics, instrumental stability, and their application to astronomy and aeronomy.



**Mary Soria** joined the Jet Propulsion Laboratory (JPL), Pasadena, CA, USA, in 1999, bringing over 15 years of experience in the assembly, tuning, and characterization of 1–24 GHz commercial monolithic microwave integrated circuit (MMIC) amplifiers. She is currently a Senior Technical Assistant with JPL. She has authored or co-authored numerous IEEE papers. Her current research interests include the microassembly of MMIC modules from 1 to 400 GHz.

Ms. Soria was a recipient of two National Aeronautics and Space Administration Tech Brief Awards.



**Mikko Varonen** (GS'09–M'10) received the M.Sc., Lic. es Sci., and D.Sc. (with distinction) degrees in electrical engineering from Aalto University (formerly Helsinki University of Technology), Espoo, Finland, in 2002, 2005, and 2010, respectively.

From 2013 to 2016, he was an Academy of Finland Post-Doctoral Researcher with the Department of Micro- and Nanosciences, Aalto University. During his post-doctoral fellowship, he was a Visiting Scientist at the Jet Propulsion Laboratory (JPL), California Institute of Technology (EE), Pasadena, CA, USA, and the Fraunhofer Institute of Applied Solid-State Physics, Freiburg, Germany. From 2013 to 2016, he was also with LNAFIN Inc., Helsinki, Finland. In 2011, he was a NASA Post-Doctoral Program Fellow at JPL. He is currently a Senior Scientist with the VTT Technical Research Center of Finland, Espoo. His current research interests include the development of millimeter-wave integrated circuits using both silicon and compound semiconductor technologies for applications ranging from astrophysics and earth remote sensing to millimeter-wave communications.



**Richard Lai** (F'10) received the Ph.D. degree from the University of Michigan, Ann Arbor, MI, USA, in 1991.

He possesses more than 25 years of experience in the research, development, and production of advanced HEMT device and monolithic microwave integrated circuit RF technologies. Since 1994, he has been the Principal Investigator of advanced HEMT research and development with Northrop Grumman Aerospace Systems, Redondo Beach, CA, USA, where he has been an Engineering Technical

Fellow since 2002. He has authored or co-authored over 200 papers, patents, and conference presentations in the area of advanced GaAs- and InP-based device and circuit technology, establishing record performance for the lowest noise amplifiers, highest frequency amplifiers, and highest power amplifiers.



**Xiaobing Mei** received the B.S. degree in physics from the University of Science and Technology of China, Hefei, China, in 1987, and the Ph.D. degree in electrical engineering from the University of California at San Diego, La Jolla, CA, USA, in 1997.

He was with Hewlett-Packard, Palo Alto, CA, USA, Agilent Technologies, Santa Clara, CA, USA, as a Senior MBE Engineer and later as an Integration Engineer. He was with Celeritek, Santa Clara, as a Senior Member of Technical Staff, leading the GaAs pHEMT development. He is currently a Senior Staff Engineer with the Micro Electronics Center, Northrop Grumman, Redondo Beach, CA, USA, leading advanced InP HEMT technology development.

Dr. Mei was a recipient of the 2012 MWCL "Tatsuo Itoh" Best Paper Award.